Materials and Devices
An International Scientific Journal
OPEN ACCESS Freely Accessible Scientific Papers.
CA-IP
Managed by scientists for Science - http://co-ac.com

Article type: A-Regular research paper

THERMAL ANNEALING IMPACT ON THE PROPERTIES OF CdSe/PbSe SUPERLATTICE THIN FILMS

C. I. ELEKALACHI (1*), I. A. EZENWA (2), N. A. OKEREKE (3), N. L. OKOLI (4), A. N. NWORI (5)

(1, 2, 3 & 5) DEPARTMENT OF INDUSTRIAL PHYSICS, FACULTY OF PHYSICAL SCIENCE, CHUKWUEMEKA ODUMEGWU OJUKWU UNIVERSITY ULI, ANAMBRA STATE, NIGERIA. ci.elekalachi@coou.edu.ng (1*), ia.ezenwa@coou.edu.ng (2), na.okereke@coou.edu.ng (3), austine2010forreal@yahoo.com (5)

(4) DEPARTMENT OF COMPUTER EDUCATION, FACULTY OF EDUCATION AND ART, MADONNA UNIVERSITY NIGERIA (OKIJA CAMPUS), ANAMBRA STATE, NIGERIA. okoli.nl@madonnauniversity.edu.ng

(4) NANO RESEARCH LABORATORY, UNIVERSITY OF NIGERIA NSUKKA, ENUGU STATE, NIGERIA.

***Corresponding author: ci.elekalachi@coou.edu.ng**

RECEIVED: 2 September 2024/ RECEIVED IN FINAL FORM: 2 November 2024 / ACCEPTED: 11 November 2024

Abstract: Superlattice thin films of CdSe/PbSe were successfully deposited on a glass substrate using successive ionic layer adsorption reaction (SILAR) method to study their properties for possible semiconductor device applications. Cadmium (II) chloride hemi (pentahydrate), lead nitrate and sodium hydrogen selenide were the precursors for Cd^{2+}, $Pb^{2+,}$ and Se^{2-} ions sources respectively. The SILAR process involved a total cycle of 100 seconds for a complete SILAR cycle with six cycles made as one layer of CdSe used as a substrate for PbSe to form CdSe/PbSe superlattice films. The deposited thin films were subjected to thermal annealing at different temperatures of 300 K, 373 K, 423 K 473 K, and 523 K and characterised for their optical, structural elemental, and morphological properties using UV-Vis spectroscopy, X-ray diffraction, and SEM/EDS techniques. The results of the optical properties showed that absorbance is high in the VIS region. At the same time, transmittance is low in the VIS region but increased to high values in the NIR region and was significantly influenced by thermal annealing. The bandgap energies of the films were found to be 1.76 eV, 1.78 eV, 1.8 eV,1.92 eV, and 2.0 eV after thermal annealing at 300 K, 373 K, 423 K, 473 K, and 523 K respectively. The XRD analysis showed that the deposited thin films are polycrystalline with diffraction spectra showing an increase in intensity at an annealing temperature of 523 K and preferential lattice planes of (101), (103), (203) attributed to CdSe and (100), (200), (220) attributed to PbSe films. The EDS results indicate that the films are composed of Cd, Pb, Se, and other traceable elements to the substrate. The SEM results showed that the CdSe/PbSe superlattice films contained agglomeration of nanorods and rice grain-shaped nanoparticles of different sizes and shapes that were found to increase with an increase in annealing temperature. These observed properties position the films for photodetector, solar cells, light-emitting diodes, photoconductors, and many other electronic and optoelectronic device applications.

Keywords: Chalcogenides, semiconductors, Bandgap, Photodetectors, Solar Cells, LEDs, SILAR

Cite this article: C. I. Elekalachi, I. A. Ezenwa, N. A. Okereke N. L. Okoli, A. N. Nwori, *OAJ Materials and Devices, Vol 8, 0211 (2024) – DOI: 10.23647/ca.md2024021*

I. Introduction

Thin film semiconductors of metal chalcogenides have demonstrated copious applications for the fabrication of many electronic and optoelectronic devices [1]. The semiconductor thin films made of chalcogenides have been greatly utilized for the fabrication of window layers for solar cells, sensor/photodetector devices, photoelectrodes, LASERs and LED devices, [2-6]. These applications have been useful in tackling many real-life problems bordering on energy, information technology and security issues. Among the metal chalcogenides (designated M-X, with M being the most metals like Cd, Cu, Fe, Ni, Zn, Pb, Mn, Co etc., while X include S, Se, Te) that have been found useful for these purposes are CdS, CdSe, CuS, CuSe, FeS, FeSe, NiS, NiSe, ZnS, ZnSe, PbS, PbSe among others [7-12]. Each of these metal chalcogenides has peculiar properties for a desired semiconducting application based on the electronic configurations of their respective elements that give rise to the groups of a semiconductor so formed [13]. Among these metal chalcogenides, CdSe and PbSe are very important group II-VI and IV-VI semiconductor materials that have shown good properties suitable for many applications including solar cells, thermoelectric cooling, optical recording, light emitting diodes, sensors, laser, thin film transistors and photoconductors, [14].

CdSe is an n-type semiconducting material with a bulk direct bandgap energy of 1.74 eV at room temperature. This bandgap energy is in the solar range and is suitable for many electronics and optoelectronics device applications including solar cells, photodetectors, light emitting diodes, Nanosensors, biomedical imaging devices, etc., [15-16]. PbSe on the other hand is a narrow bandgap semiconductor material with a bandgap energy of 0.27 eV at room temperature. This behavior results in its interesting optical, electrical, optoelectronic, and chemical stability properties for many device fabrications such as solar cells, thermoelectric cooling, optical recording, light emitting diodes, sensors, laser and thin film transistors, [17-18]. These properties of the metal chalcogenide semiconductor materials in the case of CdSe and PbSe can be changed for improved performance and wider solid-state applications through many processes such as doping, the effect of temperature, deposition method, etc., in which their physical states are transformed. For instance, the phenomenon of the quantum confinement effect has shown the tuning of the bandgap energy of most chalcogenides' materials to a higher effective energy region for absorbing maximum intensity over the solar radiation spectrum suitable for more device applications, [19]. The effect of thermal annealing on the electrical behaviour of CdS/PbSe thin films deposited by the aqueous chemical deposition method has been reported by [20] to change from an ohmic to diode response by applying thermal annealing at 150 oC for 5 min according to their I-V characterization on the film samples. The properties of CdSe thin films deposited by solution growth technique (SGT) at 80 °C bath temperature reported by [21] have shown to be blue shifted as a result of the deposition condition demonstrating good photo response suitable for photosensor applications. [22] studied the effect of different Zn concentrations on CdSe thin films deposited by the Electron Beam Evaporation method and reported that the bandgap energy of the films increased with an increase in the Zn concentration and other properties such as structural parameters and electrical resistivity were also influenced. The thin films of CdSe and (Fe, Mn) doped CdSe deposited by the electrodeposition method have also been reported by [23] to show an increase in the conversion efficiency as a result of doping with Mn and Fe ions concentrations and inferred that the deposited thin films can be used for solar cell and photoelectrochemical (PEC) cell materials fabrications.

In this report, we studied the properties of superlattice thin films of CdSe/PbSe fabricated using the SILAR method and annealed at different temperatures to determine their properties for their possible application in optoelectronic devices.

II. Materials and Method

II.I. Method

The materials used for the deposition of the CdSe/PbSe superlattice thin films are; cadmium (II) chloride, Lead (II) nitrate, selenium dioxide, sodium borohydride, acetone, nitric acid and distilled water. Laboratory apparatus and equipment used are; Digital weighing balance, Glass beakers (100 mL, 250 mL and 500 ml), Measuring cylinder (50 mL and 100 mL), Microscopic glass slides (substrates) of dimension (25.4 mm, 76.2 mm, 1.2 mm), Plastic sample holders (substrates rack), Magnetic stirrer with hot plate and Electric oven for sample annealing.

II.II. Experimental Procedure

The materials (reagents) are of analytical grade and were used as obtained. The molar solutions of the reagents were prepared and used for the depositions using the general equation (1) for reacting mass

$$Reacting\ Mass = \frac{molarity \times \text{molar mass} \times volume}{1000} \quad (1)$$

0.2 M of Cadmium (II) chloride hemi(pentahydrate) and 0.2 M of lead nitrate were prepared by dissolving 22.84 g and 33.12 g of the compounds respectively in 500 mL of distilled water. These prepared solutions of the compounds served as precursors for Cd2+ and Pb2+. Sodium hydrogen selenide used as the precursor for selenium ion was prepared by a reaction between sodium borohydride and selenium (IV) oxide at room temperature. The reaction involves a mixture of 40 mL of 0.05 M of selenium (IV) oxide with 40 mL of 0.03 M of sodium borohydride. The solution was freshly prepared before its use regarding its unstable nature. The superlattice thin films of CdSe/PbSe were grown on the glass substrate using the successive ion layer adsorption reaction (SILAR) method. Four beakers were used with the first beaker labelled beaker A containing cationic precursors, the second beaker labelled beaker B containing ionic exchange medium (distilled water), and beaker C containing anionic precursors while the last beaker labelled D contained ionic exchange medium. The SILAR process with a total cycle time of 100 seconds involves the following four steps:

(i) Immersion of the cleaned substrate in the first reaction beaker (A) containing Cd^{2+} precursor solution for 40 seconds to absorb Cd^{2+} on the surface of the substrate.

(ii) This substrate was rinsed in high-purity distilled water for 10 seconds to remove excess Cd^{2+} that was loosely adherent to the glass substrate (achieved in the previous step).

(iii) The substrate was then immersed in the anionic precursor solution of freshly prepared NaHSe for 40 seconds. The selenide (Se^{2-}) ions reacted with the absorbed Cd^{2+} on the active centre of the substrate to form metal Selenide films.

(iv) Again, the substrate was rinsed in distilled water for 10 seconds to remove loosely bound ions present on the substrate and unreacted cations and anions and this completed one cycle.

The above process was repeated six times and completed one layer of the superlattice films. The layered films of CdSe on the substrate were thereafter used to repeat the SILAR process by immersing in the beaker (A) that contains the Pb^{2+} precursor. The processes and number of cycles were repeated and complete superlattice thin films of CdSe/PbSe were fabricated on the glass substrate. Five samples of the CdSe/PbSe thin films were fabricated and annealed at different temperatures as depicted in Table 1.

Table 1: Optimization of annealing temperature for CdSe/ PbSe thin films

Sample name	Number of SILAR Layers		Annealed temp. for 60 minutes (K)
	Layer I (CdSe)	Layer 2 (PbSe)	
$(CdSe/PbSe)_1$	6	6	300
$(CdSe/PbSe)_2$	6	6	373
$(CdSe/PbSe)_3$	6	6	423
$(CdSe/PbSe)_4$	6	6	473
$(CdSe/PbSe)_5$	6	6	523

The unannealed and annealed CdSe/PbSe films were characterized for their optical, structural, compositional and morphological properties using a spectrophotometer (model: 756S UV – VIS), Bruker D8 high-resolution diffractometer, MIRA TESCAN SEM and Nova Nano SEM respectively

III. Results

III.I. Thin Film Thickness Study

The physical properties of the deposited CdSe/PbSe superlattice thin films that were used to calculate film thicknesses for growth parameters of annealing temperature and the number of SILAR cycles respectively are presented in Table 2. The thicknesses (t) of the deposited thin films were evaluated using the gravimetric method as given by [24-28].

$$t = \frac{\Delta m}{\rho A} \quad (2)$$

where Δm is the mass of the film, A is the surface area of the deposited film and ρ is the bulk density of the material film. The masses of the deposited films were obtained by finding the difference in mass between the mass of the glass substrate after the film deposition and its mass before the film deposition. Figure 1 shows the variation of annealing temperature with thickness of the deposited CdSe/PbSe superlattice thin films. The CdSe/PbSe superlattice thin films annealed at different temperatures from 300 K to 523 K showed that the film thickness increased from 114.531 nm to 206.156 nm. This result showed that the thickness of the superlattice films increased as the annealing temperature increased.

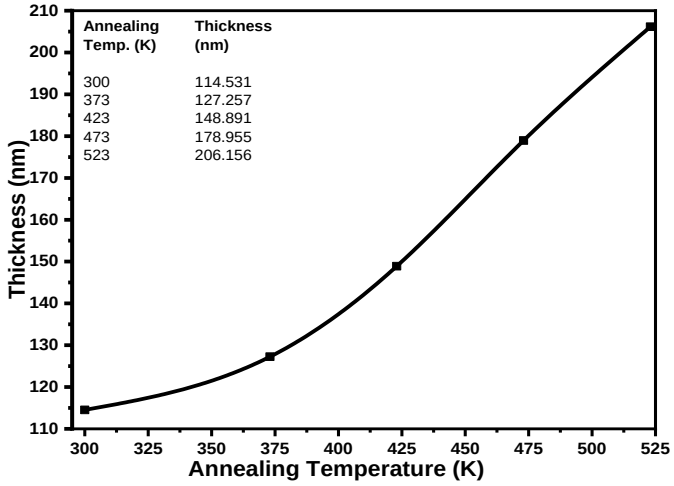

Figure 1: Film thickness plotted against annealing temperature for SILAR deposited Cadmium selenide/lead selenide superlattice

III.II. Optical Properties of the Films

Figure 2 is the graph of absorbance against wavelength for the deposited CdSe/PbSe superlattice thin films annealed at different temperatures to determine the effect of heat treatment on the optical properties of the films. The graph showed that the absorbance of the films increased with an increase in the annealing temperatures, with the films annealed at 523 K and 300 K having the highest and lowest absorbance values respectively throughout the UV, VIS and NIR regions. The absorbance is observed to be higher in the VIS region for all the films and decreases in the NIR region. The maximum values of 0.3, 0.375, 0.45, 0.70 and 0.75 occurred at a wavelength of 400 nm for the films 300 K, 373 K, 423 K, 473 K and 523 K respectively. These results showed that annealing improves the absorbance property of the fabricated thin films of CdSe/PbSe for desired applications.

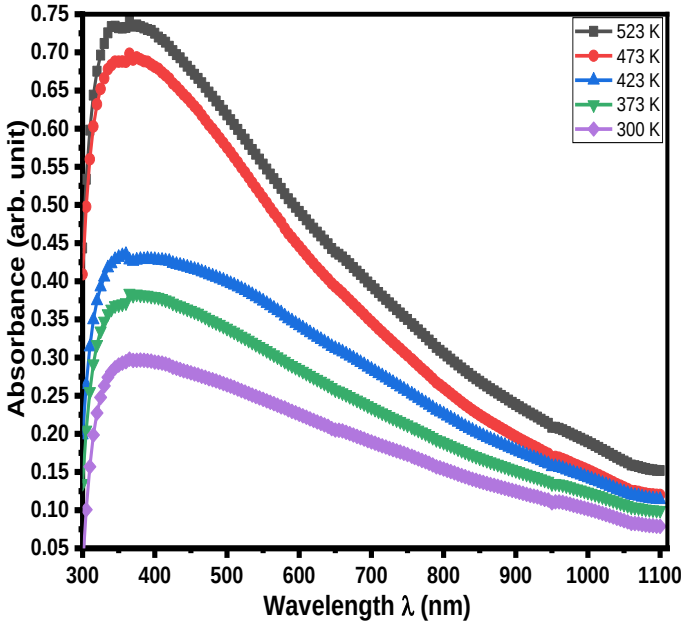

Figure 2: Graph of absorbance against wavelength for the CdSe/PbSe thin film

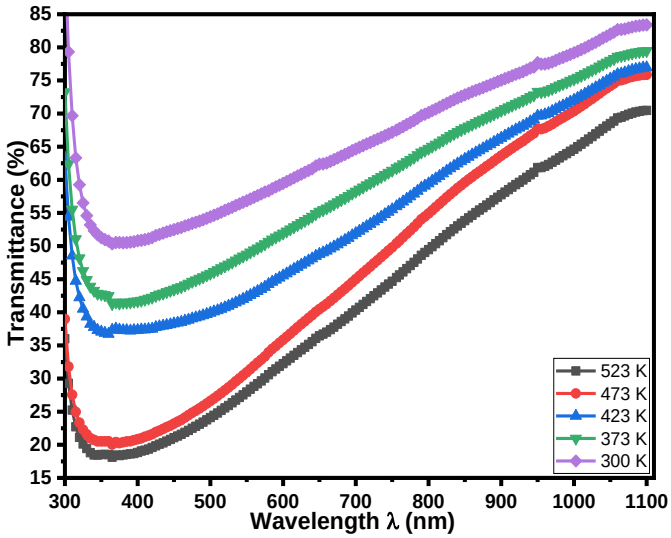

Figure 3: Graph of Transmittance (%) against wavelength for CdSe/PbSe thin film

Figure 3 shows the graph of the percentage transmittance of the films of CdSe/PbSe annealed at different temperatures. The transmittance was evaluated using the relationship between absorbance and transmittance as follows [29].

$$T = 10^{-A} \quad (3)$$

Where A is the measured absorbance of the films from the spectrophotometer machine.

The figure showed that the transmittance of the films decreased with an increase in annealing temperature. The transmittance however increases with wavelength suggesting higher transmittance in the NIR region of the electromagnetic spectrum (EMS). The film annealed at 523 K has the highest transmittance in the range of 52.50 % - 85 % while the film annealed at 300 K has the lowest transmittance in the range of 17.50 % - 72.50 % within the VIS and NIR regions of EMS. The high transmittance exhibited by films in the NIR region positions them for window coating in the low temperate regions of the world for in-house heating and anti-reflection coating applications.

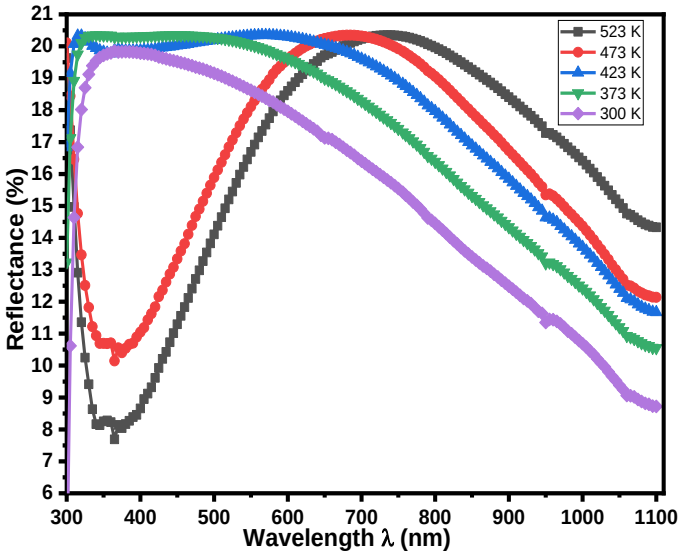

Figure 4: Graph of Reflectance (%) against wavelength for CdSe/PbSe thin film

Figure 4 is the graph of reflectance against wavelength for the fabricated superlattice films CdSe/PbSe annealed at different temperatures. The reflectance R of the films was calculated using the conservation law for radiant energy relating absorbance, transmittance and reflectance as given by [30 - 32].

$$A + T + R = 1. \quad (4)$$

Where A and T are the absorbance and transmittance of the films respectively.

The graph showed that the films have low reflectance (with maximum reflectance of 20 %). The reflectance increased with annealing temperature in the NIR region while in the VIS region, it initially increased with annealing temperature up to 423 K and thereafter decreased to lower percentage values at annealing temperatures of 473 K and 523 K. The reflectance of the films decreases with an increase in wavelength except for the films annealed at 473 K and 523 K which increased with the wavelength in the VIS and then decreased in the NIR region. The low reflectance of the films positions them for anti-reflection coating applications.

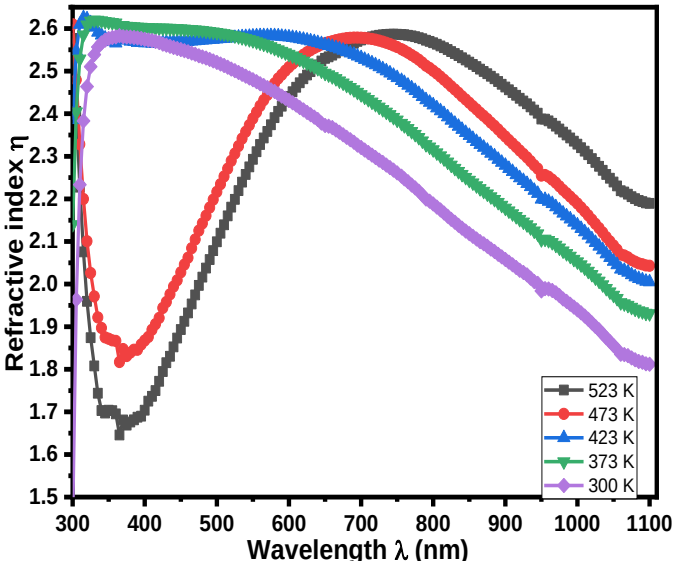

Figure 5: Graph of Refractive index against wavelength for CdSe/PbSe thin film

The graph of refractive index as a function of wavelength for the fabricated thin films of CdSe/PbSe is presented in figure 5. The refractive index of the films was evaluated using the relation given by [33-36].

$$\eta = \frac{1+R}{1-R} + \sqrt{\frac{4R}{(1-R)^2} - k^2} \quad (5)$$

Where R is the reflectance of the films

The refractive index of the films followed the same pattern as reflectance and has a maximum value of 2.6 in the VIS region. The films have a high refractive index value and increase with an increase in annealing temperatures up to the temperature of 423 K and then decrease to lower values at annealing temperatures of 473 K and 523 K in the VIS region. The refractive index of the films also generally decreased with an increase in wavelength except for the films annealed at 473 K and 523 K which showed an increase in the refractive index values as wavelength increased in the VIS region of EMS.

The extinction coefficient (k) of the deposited thin films was calculated using the relation as given by [37-38].

$$k = \frac{\alpha\lambda}{4\pi}. \quad (6)$$

Where k is called the extinction coefficient or attenuation constant of the film.

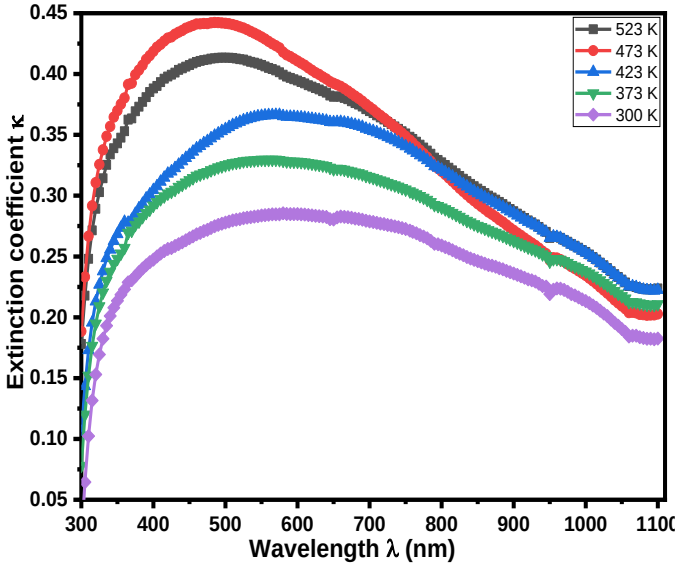

Figure 6: Graph of Extinction coefficient against wavelength for the CdSe/PbSe thin film

Figure 6 is the graph of the extinction coefficient against wavelength for the deposited thin films annealed at different temperatures. From the graph, the extinction coefficient of the films is observed to increase with an increase in annealing temperature up to 473 K and thereafter decrease to a lower value as the annealing temperature increases to 523 K. The extinction coefficient of the films is generally low but increased to the maximum values in the mid-VIS region and then decreased in the NIR regions of EMS.

The plots of $(\alpha h\upsilon)^2$ against photon energy to determine the bandgap energies of the fabricated thin films of CdSe/PbSe at different annealing temperatures are presented in figure 7. The optical bandgap energy of the superlattice thin films was calculated using the relation according to [39].

$$\alpha h\upsilon = A(h\upsilon - E_g)^r \qquad (7)$$

Where h is Planck's constant and r =1/2 for direct allowed transition and r = 3/2, for forbidden transition, υ is the frequency, A is constants and E_g is the optical bandgap energy.

The energy bandgaps of each of the films extrapolated on the photon energy axis at $(\alpha h\upsilon)^2 = 0$ are observed to be 1.76 eV, 1.78 eV, 1.8 eV,1.92 eV and 2.0 eV for the films annealed at 300 K, 373 K, 423 K, 473 K and 523 K respectively. These values of bandgap energies are in the visible spectrum and as such the films can be used for photovoltaic cell device development for solar energy harnessing.

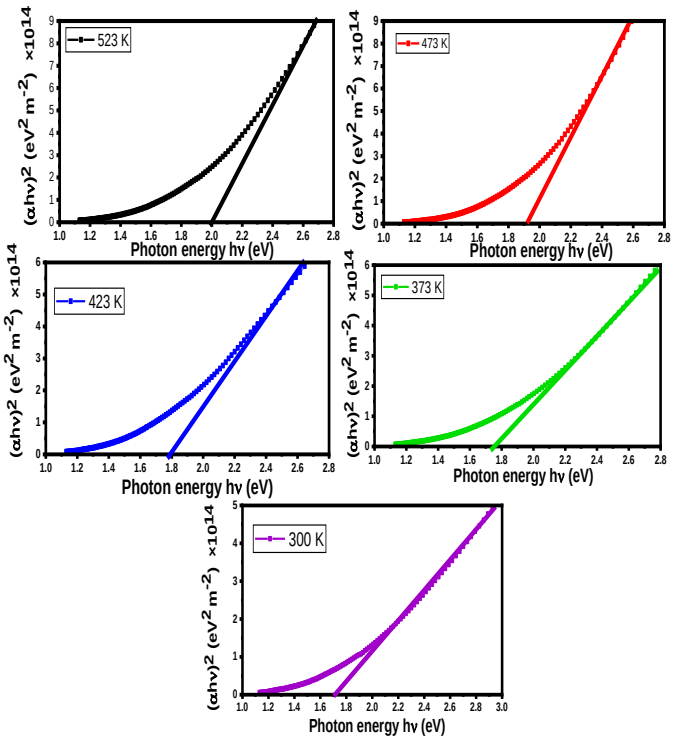

Figure 7: Plots of $(\alpha h\upsilon)^2$ against photon energy for the CdSe/PbSe thin film

III.III. Structural Analysis of the CdSe/PbSe Thin Films

Figure 8 presents the X-ray diffraction patterns of the as-deposited CdSe/PbSe thin film and those annealed at 423 K and 523 K. No prominent peak was observed for CdSe/PbSe thin film deposited at 300 K. Diffractogram of the deposited CdSe/PbSe thin films annealed at 423K and 523 K showed peaks corresponding to the hexagonal and cubic phase of cadmium selenide and lead selenide respectively. Four peaks correspond to standard Powder Diffraction File (PDF) card number 01-077-2307 for hexagonal CdSe while two peaks correspond to the peaks in the standard PDF card number 01-077-0245 for PbSe. The diffraction spectra showed an increase in intensity at an annealing temperature of 523 K. The result also showed that the deposited thin films are polycrystalline. The structural parameters of the deposited thin films are presented in Table 2. The XRD patterns show that the intensity of the peaks increases with annealing temperature, indicating an improvement in crystallinity. Higher peak intensities at higher annealing temperatures suggest enhanced crystal growth and better-defined crystalline structures.

The average grain size (D), dislocation density (δ) and micro-strain (ε) of the films were calculated using Scherrer's formula and Williamson & Smallman's equations given by [40 - 41].

$$D = \frac{k\lambda}{\beta\cos\theta} \qquad (8)$$

$$\delta = \frac{1}{(D)^2} \quad (9)$$

$$\varepsilon = \frac{\beta \text{Cos}\theta}{4} \quad (10)$$

where **β**, θ, k and λ are full width at half maximum (FWHM), Bragg's angle, constant and X-ray wavelength respectively.

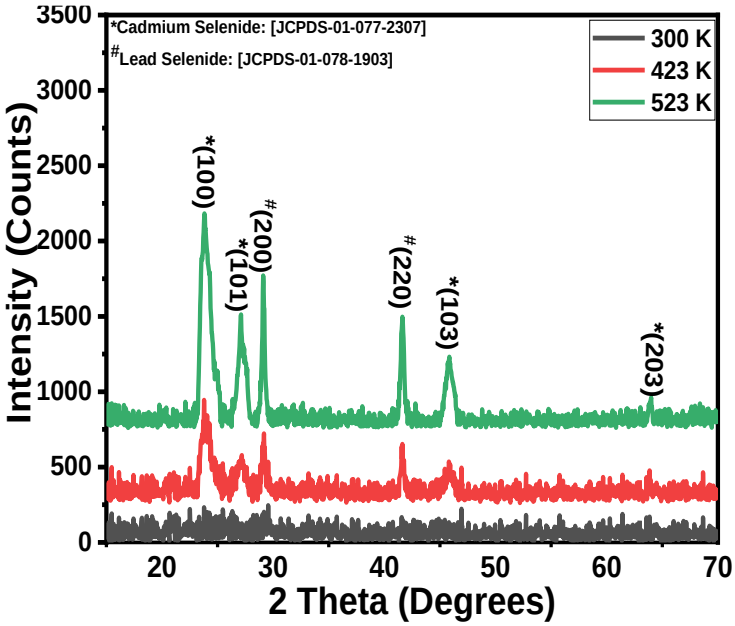

Figure 8: XRD pattern of the deposited CdSe/PbSe thin films annealed at 300 K, 423 K and 523 K

Table 2: Crystal-structural properties of CdSe/PbSe thin films annealed at 423 K and 523 K

Samples	Observed		(hkl)	FWHM (°)	Crystallite Size (nm)	$\delta \times 10^{15}$ lines/m²	$\varepsilon \times 10^{-3}$
	2θ (°)	D-spacing (Å)					
423 K	23.975*	3.709	100	1.053	8.053	15.42	21.65
	27.133*	3.284	101	0.712	11.989	6.9575	12.87
	29.146#	3.061	200	0.432	19.852	2.5375	7.248
	41.622#	2.168	220	0.36	24.675	1.6425	4.13
	45.808*	1.979	103	0.471	19.114	2.7372	4.867
			Average		**16.736**	**5.859**	**10.150**
523 K	23.947*	3.713	100	1.028	8.252	14.685	21.147
	27.176*	3.279	101	0.821	10.402	9.243	14.815
	29.120#	3.064	200	0.315	27.255	1.346	5.284
	41.620#	2.168	220	0.372	23.869	1.755	4.269
	45.852*	1.977	103	0.797	11.304	7.826	8.222
	63.876*	1.456	203	0.092	106.508	0.088	0.643
			Average		**31.265**	**5.824**	**9.063**

The average crystallite size of the film annealed at 423 K was found to be 16.934 nm. The increase in crystallite size with annealing temperature indicates that higher temperatures promote the growth of larger crystallites. This growth is due to the enhanced mobility of atoms at higher temperatures, allowing them to occupy more energetically favorable positions in the crystal lattice. The dislocation density and micro-strain of the film were found to be $5.859 \times 10^{15}\ lines/m^2$ and 10.150×10^{-3} respectively. The average crystallite size of the film annealed at 523 K was found to be 31.265 nm while the dislocation density and micro-strain of the film were found to be $5.824 \times 10^{15}\ lines/m^2$ and 9.063×10^{-3} respectively. The XRD analysis of CdSe/PbSe thin films annealed at 300 K, 423 K, and 523 K reveals that annealing significantly enhances the crystalline quality of the films. Higher annealing temperatures promote the growth of larger crystallites, reduce dislocation density, and relax lattice strains. These improvements in structural properties are critical for the potential applications of these thin films in optoelectronic devices, where high crystallinity and low defect densities are essential for optimal performance.

III.IV. Compositional Analysis of the CdSe/PbSe Thin Film

Figure 9 shows the EDS graphs of the deposited CdSe/PbSe superlattice thin films at 300 K and those annealed at 423 K and 523 K. The atomic percentages of the elements present in the deposited thin films were presented along with the EDS spectra. The EDS spectra confirmed the presence of cadmium (Cd), lead (Pb), selenium (Se) and other elements such as carbon (C), oxygen (O), sodium (Na), Magnesium (Mg), silicon (Si) and calcium (Ca). These other elements may be due to the composition of the microscopic glass used for the deposition. A non-linear relationship was also observed in atomic percentages of cadmium, lead and selenium as the annealing temperature increased from a room temperature of 300 K to an annealing temperature of 523 K.

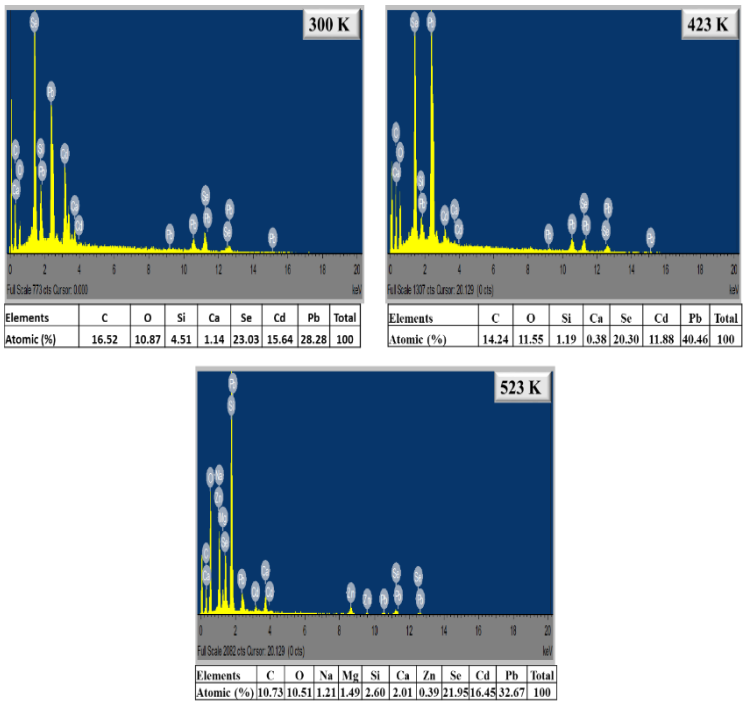

Elements	C	O	Si	Ca	Se	Cd	Pb	Total
Atomic (%)	16.52	10.87	4.51	1.14	23.03	15.64	28.28	100

Elements	C	O	Si	Ca	Se	Cd	Pb	Total
Atomic (%)	14.24	11.55	1.19	0.38	20.30	11.88	40.46	100

Elements	C	O	Na	Mg	Si	Ca	Zn	Se	Cd	Pb	Total
Atomic (%)	10.73	10.51	1.21	1.49	2.60	2.01	0.39	21.95	16.45	32.67	100

Figure 9: EDS spectra of the deposited cadmium selenide/lead selenide (CdSe/PbSe) superlattice thin films annealed at 300 K, 423 K and 523 K

III.V. Morphological Properties of the Thin Films

Figure 10 showed SEM images of as-deposited CdSe/PbSe superlattice thin film annealed at 300 K, 423 K and 523 K. The SEM images of CdSe/PbSe thin films annealed at 300 K, 423 K, and 523 K reveal significant morphological changes with increasing temperature. At 300 K, the particles display a relatively uniform distribution with well-defined shapes and some agglomeration, featuring a mixture of smaller and larger particles. As the temperature increases to 423 K, the particles become more aggregated, with a decrease in the distinctness of individual particle boundaries, indicating some degree of sintering or fusion. The surface texture also appears rougher and more interconnected. At 523 K, the aggregation is even more pronounced, with particles forming a continuous network, resulting in a significantly rougher surface where distinct particle boundaries are less visible. These observations suggest that particle size increases and surface area decreases with higher temperatures due to sintering effects. The morphological transformation from discrete particles at 300 K to more fused structures at higher temperatures likely enhances mechanical strength and thermal stability but may impact conductivity. The SEM findings, consistent with XRD results show increased crystallite size, reduced dislocation density, and improved

crystallinity, underscore the importance of annealing in optimizing thin film properties for optoelectronic applications.

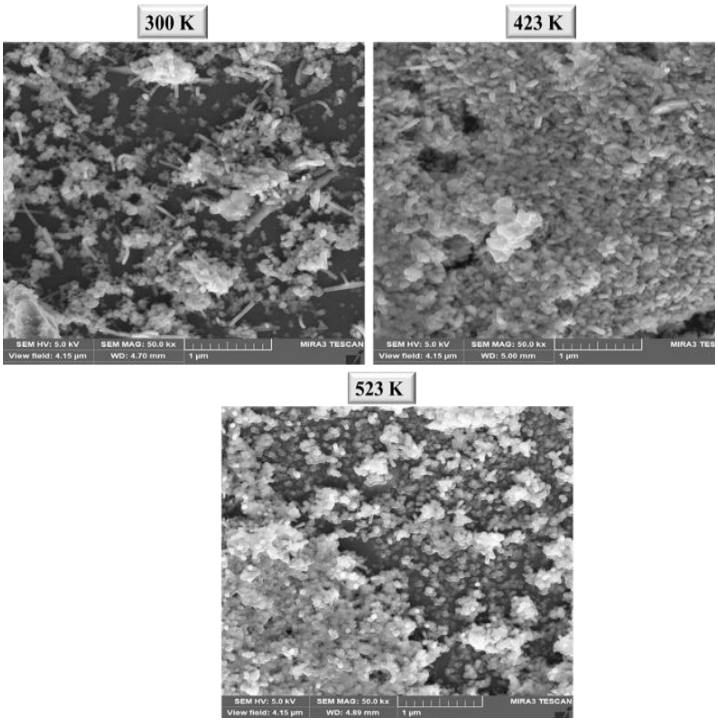

Figure 10: SEM images of SILAR deposited CdSe/PbSe superlattice thin films at 300 K, annealed at 423 K and 523 K

Conclusion

The results of the characterizations of the deposited superlattice thin films of CdSe/PbSe showed that the optical properties of the films like absorbance are generally influenced by thermal annealing and are higher in the VIS region than in the NIR region. The transmittance of the films increased to high values in the NIR region while the reflectance and extinction coefficient were low in the VIS/NIR regions but were improved as a result of annealing. The bandgap energy of the films was found to be 1.76 eV, 1.78 eV, 1.8 eV,1.92 eV and 2.0 eV for the films annealed at 300 K, 373 K, 423 K, 473 K and 523 K respectively. The XRD results indicate that the deposited thin films of CdSe/PbSe are polycrystalline with diffraction spectra showing an increase in intensity as the annealing temperature increased to 523 K, an indication of enhancement in crystallinity of CdSe/PbSe superlattice thin films. The average crystallite size of the film annealed at 423K and 523 K was found to be 16.734 and 31.265 nm while the dislocation density and micro-strain of the film are 5.824×10^{15} lines/m^2 and 5.859×10^{15} lines/m^2. The micro-strain of the films was found to be 1.015×10^{-2} and 9.063×10^{-3} respectively. The EDS analysis confirmed the presence of cadmium (Cd), lead (Pb), selenium (Se) and other elements like carbon (C), oxygen (O), sodium (Na), Magnesium (Mg), silicon (Si) and calcium (Ca) traceable to the composition of the microscopic glass used for the film's deposition. SEM images of CdSe/PbSe thin films annealed at 300 K, 423 K, and 523 K, showed increased particle aggregation and rougher surfaces with higher temperatures due to sintering effects. These morphological changes, consistent with XRD results, enhance the properties of the thin film thereby highlighting the importance of annealing for optimizing thin film properties for optoelectronic applications. These properties exhibited by the deposited thin films of CdSe/PbSe indicate that they are in a good position for photodetector, solar cells, light emitting diodes, photoconductors and many other electronic and optoelectronic applications.

Acknowledgement

We are deeply grateful to the staff of the Nanotech Research Laboratory, Department of Physics and Astronomy, University of Nigeria Nsukka, Enugu State, Nigeria, for their assistance with the optical analysis of our samples. We also acknowledge the team of scientists from the Material Research Department, Themba Labs, Johannesburg, South Africa, and the Electron Microscope Unit, University of Cape Town, South Africa, for their help in conducting the structural and compositional SEM analysis in their laboratories.

Funding/Competing Interests

The authors declare they have no competing financial or non-financial interests of any kind relevant to the content of this article. The authors declare that no funds, grants, or other support were received during the preparation of this manuscript.

Compliance with Ethical Standards

This article does not involve any experiments with human participants or animal subjects. The authors declare that they have no known competing financial interests or personal relationships that would influence the work reported in this paper

Author's Contributions

All authors contributed to the study's conception and design. Material preparation, experiments, data collection and analysis were performed by **Elekalachi, C. I., Okoli, N. L. and Nwori, A. N.** The first draft of the manuscript was written by **Elekalachi C. I., Okoli N. L and Nwori, A. N. Ezenwa, I. A., Okereke, N. A and Okoli, N. L.** participated in the discussion and gave some valuable suggestions. **Elekalachi, C. I., Ezenwa, I. A., Okereke N. A and Nwori, A. N.** revised the manuscript before submission. All authors read and approved the final version of the manuscript.

REFERENCES

[1] T.M. Emeakaroha, B.A. Ezekoye, V.A. Ezekoye, K.O. Ighodalo. "Optical and Structural Properties of Silar-Grown Highly Oriented Lead Sulphide (PbS) Thin Films." *Chalcogenide Letters* 13, no. 3 (2016): 91-96.

[2] E.K. Nasr El Din, M.O. Dawood, A.M. Ali. "Influence of Thickness on Structural and optical properties of the CdS single crystal nanostructure thin films Deposited Via Thermal evaporation." *Tikrit Journal of Pure* Science 24, no. 6 (2019): 98-103. Available from: http://dx.doi.org/10.25130/tjps.24.2019.114

[3] U. Khairnar, S. Behere, P. Pawar. "Optical Properties of Polycrystalline Zinc Selenide Thin Films." *Materials Sciences and Applications* 3, (2012): 36-40. Available from: http://dx.doi.org/10.4236/msa.2012.31006

[4] M.F. Hasaneen, Z.A. Alrowaili, W.S. Mohamed. "Structure and optical properties of polycrystalline ZnSe thin films: validity of Swanepol's approach for calculating the optical parameters." *Material Research Express* 7, no. 016422 (2020): 1-15. Available from: https://doi.org/10.1088/2053-1591/ab6779

[5] T. Lakshmikandhan. "Synthesis of ZnSe thin film by chemical bath deposition and for photovoltaic application." *Malaya Journal of Matematik* 5, no. 2 (2020): 2237-2239. Available from: https://doi.org/10.26637/MJM0S20/0575

[6] N. Loudhaief, M.B. Salem, M. Zouaoui. "Structural, Optical and Electrical Properties of Eu-doped CuS Nanoparticles Synthesized Through the Aqueous Route." *Engineering Physics* 1, no. 4 (2020): 7-14. Available from: doi:10.11648/j.ep.20200401.12

[7] M.T. Chowdhury, M.A. Zubair, H. Takeda, K.M.A. Hussain, M.F. Islam. "Optical and structural characterization of ZnSe thin film fabricated by thermal vapour deposition technique." *AIMS Materials Science* 4, no. 5 (2017): 1095-1121. Available from: http://www.aimspress.com/journal/Materials

[8] J.P. Tailor, S.H. Chaki, M.P. Deshpande. "Comparative study between pure and manganese doped copper sulphide (CuS) nanoparticles." *Nano Express* 2, (2021): 1-11. Doi: https://doi.org/10.1088/2632-959X/abdc0d

[9] O.C. Olatunde, D.C. Onwudiwe. "Temperature Controlled Evolution of Pure Phase Cu9S5 Nanoparticles by Solvothermal Process." *Frontiers in Materials* 8, (2021): 1-7. Available from: Doi: http://dx.doi.org/10.3389/fmats.2021.687562

[10] A.D. Dhondge, S.R. Gosavi, N.M. Gosavi, C.P. Sawant, A.M. Patil, A.R. Shelke, N.G. Deshpande. "Influence of Thickness on the Photosensing Properties of Chemically Synthesized Copper Sulfide Thin Films." *World Journal of Condensed Matter Physics* 5, (2015): 1-9. Available from: Doi: http://dx.doi.org/10.4236/wjcmp.2015.51001

[11] A.A. Kadhim, E.I. Abdul-Majeed, M.M. Jassim. "Structural and Optical Properties of PbS Thin Films Deposited by Pulsed Laser Deposited (PLD) Technique at Different Annealing Temperature." *International Journal of Physics* 5, no. 1 (2017): 1-8. Available online at http://pubs.sciepub.com/ijp/5/1/1

[12] S. Thirumavalavan, K. Mani, S. Sagadevan. "Investigation of the Structural, Optical and Electrical Properties of Copper Selenide Thin Films." *Materials Research* 18, no. 5 (2015): 1000-1007. Doi: http://dx.doi.org/10.1590/1516-1439.039215

[13] S.T.N. Narayana, H.L. Pushpalatha, R. Ganesha. "Synthesis of CdSe Thin Film by Chemical Bath Deposition and Characterization." *International Journal of Engineering Science and Innovative Technology (IJESIT*) 6, no. 1 (2017): 41-49.

[14] M.A. Alvi, Z.H. Khan. "Synthesis and characterization of nanoparticle thin films of a-(PbSe)100−xCdx lead chalcogenides." *Nanoscale Research Letters* 8, no. 148 (2013): 1-10. Available from: http://www.nanoscalereslett.com/content/8/1/148

[15] S. Hussain, M. Iqbal, A.A. Khan, M.N. Khan, G. Mehboob, S. Ajmal, J.M. Ashfaq, G. Mehboob, M.S. Ahmed, S.N. Khisro, C.J. Li, R. Chikwenze, S. Ezugwu S. "Fabrication of Nanostructured Cadmium Selenide Thin Films for Optoelectronic

Applications." *Frontier in Chemistry* 9, (2021): 661723. Available from: Doi: http://dx.doi.org/10.3389/fchem.2021.661723

[16] N. Gopakumar, P.S. Anjana, P.K.V. Pillai. "Chemical Bath Deposition and Characterization of CdSe Thin Films for Optoelectronic Applications." *Journal of Materials Science* 45, (2010): 6653–6656. Available from: Doi: http://dx.doi.org/10.1007/s10853-010-4756-1

[17] S. Peng, H. Li, C. Zhang, J. Han, X. Zhang, H. Zhou, X. Liu, J. Wang. "Promoted Mid-Infrared Photodetection of PbSe Film by Iodine Sensitization Based on Chemical Bath Deposition." *Nanomaterials*, 12, no. 1391 (2022): 1-13. Available from https://doi.org/10.3390/nano12091391

[18] S.M. Ho, A. Kassim, A.H. Abdullah, S. Nagalingam, S. "XRD, AFM and UV-Vis optical studies of PbSe thin films produced by chemical bath deposition method." *Transactions C: Chemistry and Chemical Engineering* 17, no. 2 (2010): 139-143.

[19] S. Abe. "One-step Synthesis of PbSe-ZnSe Composite Thin Film." *Nanoscale Research Letters* 6, no. 324 (2011): 1-6. Available from http://www.nanoscalereslett.com/content/6/1/324

[20] J.A. Heredia-Cancino, O. Salcido, R. Britto-Hurtado, S.G. Ruvalcaba-Manzo, R. Ochoa-Landín, S.J. Castillo. "CdS/PbSe Heterojunction Made via Chemical Bath Deposition and Ionic Exchange Processes to Develop Low-Cost and Scalable Devices." *Applied Science* 11, (2021): 1-11. Available from: https://doi.org/10.3390/app112210914

[21] H.K. Sadekar, A.V. Ghule, R. Sharma. "Fabrication of CdSe Thin Film for Photosensor Applications." *International Journal of Innovation in Engineering and Technology* 5, no. 1 (2015): 35-41.

[22] S. Rani, J. Shanthi, M. Kashif, A. Ayeshamariam, M. Jayachandran. "Studies on Different Doped Zn Concentrations of CdSe Thin Films." *Journal of Powder Metallurgy & Mining* 5, no. 1 (2016): 1-7. Available from: doi:10.4172/2168-9806.1000143

[23] S.K. Shinde, D.P. Dubal, G.S. Ghodake, V.J. Fulari. "Electronic impurities (Fe, Mn) doping in CdSe nanostructures for improvements in photoelectrochemical applications." *Royal Society of Chemistry* 4, no. 63 (2014): 33184-33189. Available from: https://doi.org/10.1039/C4RA02791D

[24] F. Gode, A. Kariper, E. Guneri, S. Unlu. "Effect of Complexing Agents on the Structural, Optical and Electrical Properties of Polycrystalline Indium sulphide Thin Films deposited by Chemical Bath Method." *Acta physica polonica A* 132, no. 3 (2017): 527-530. Available from: http://doi.org/10.12693/APhysPolA.132.527

[25] F. Gode, S. Unlu. "Nickel doping effect on the structural and optical properties of indium sulfide thin films by SILAR." *Open Chemistry* 16, (2018): 757-762. Available from http://dx.doi.org/10.1515/chem-2018-0089

[26] P. Chaudhary, V. Kumar. "Preparation of ZnO thin film using sol-gel dip-coating technique and their characterization for optoelectronic applications." *World Scientific News* 121, (2019): 64-71. Available online at www.worldscientificnews.com

[27] L.N. Ezenwaka, N.L. Okoli, N.A. Okereke, I.A. Ezenwa, A.N. Nwori. "Properties of Electrosynthesized Cobalt Doped Zinc Selenide Thin Films Deposited at Varying Time." *Nanoarchitectonic* 3, no. 1 (2022): 1-17. Available from: https://doi.org/10.37256/nat.3120221040

[28] K. Ravi, V. Chitra. "Structural and Surface morphology of Lead Selenide (PbSe) thin films." *IOP Conference Series: Materials Science and Engineering* 932, (2020): 1-8. Available from: doi:10.1088/1757-899X/932/1/012133

[29] A.N. Nwori, L.N. Ezenwaka, I.E> Ottih, N.A. Okereke, S.N. Umeokwona, N.L. Okoli, I.O. Obimma. "Study of the Optical and Solid-State Properties of Copper Manganese Sulphide (CuMnS) Thin Film Semiconductors for Possible Optoelectronics Applications." *Journal of Physics and Chemistry of Materials* 8, no. 3 (2021): 23-33.

[30] R.O. Ijeh, A.C. Nwanya, A.C. Nkele, I.G. Madiba, Z. Khumalo, A.K.H. Bashir, R.U. Osuji, M. Maaza, F.I. Ezema. "Magnetic and Optical Properties of Electrodeposited Nanospherical Copper Doped Nickel Oxide Thin Films." *Physica E: Low-dimensional Systems and Nanostructures* 113, (2019): 233-239. Available from: https://doi.org/10.1016/j.physe.2019.05.013

[31] M.H. Shinen, S.A.A. Alsaati, F.Z. Rasooqi. "Preparation of high transmittance TiO2 thin films by Sol-gel Techniques as antireflection coating." *Journal of Physics, Conference Series* 1032, (2018): 1-11. Available from: http://dx.doi.org/10.1088/1742-6596/1032/1/012018

[32] S.A.J. Al – Dahaan, A.H.O. Al-khayatt, M.K. Salman. "The optical Properties of Fe2O3 Thin Film Prepared by Chemical spray pyrolysis Deposition (CSP)." *Journal of Kufa-Physics* 6, no. 2 (2014): 16-23.

[33] E. Guneri, A. Kariper. "Characterization of high-quality Chalcogenide thin films fabricated by Chemical Bath Deposition." *Electronic Materials Letters* 9, no. 1 (2013): 13-17. Available from:https://doi.org/10.1007/s13391-012-2099-6

[34] C. Augustine, M.N. Nnabuchi, R.A. Chikwenze, F.N.C. Anyaegbunam, P.N. Kalu, B.J. Robert, C.N. Nwosu, C.O. Dike, E.N. Taddy. "Comparative investigation of some selected properties of Mn3O4/PbS and CuO/PbS composites thin films." *Material Research Express* 6, (2019): 1-10.

[35] I. A. Kariper. "Synthesis and Characterization of CrSe Thin Film Produced via Chemical Bath Deposition." *Optical Review* 24, no. 2 (2017): 139-146. Available from:https://doi.org/10.1007/s10043-017-0307-1

[36] I. A. Kariper. "A new Route to Synthesis MnSe Thin films by Chemical Bath Method." *Material Research* 21, no. 2 (2018): 1-6. Available from: http://dx.doi.org/10.1590/1980-5373-MR-2017-0215

[37] N.O. Ongwen, A.O. Oduor, E.O. Ayieta. "Effect of Concentration of Reactants on the Optical Properties of Iron-Doped Cadmium Stannate Thin Films Deposited by Spray Pyrolysis." *American Journal of Materials Science* 9, no. 1 (2019): 1-7. Available from: doi:10.5923/j.materials.20190901.01

[38] P. Sreedev, V. Rakhesh, N.S. Roshina. "Optical Characterization of ZnO thin Films Prepared by Chemical Bath Deposition Method." *IOP Conf. Series: Materials Science and Engineering* 377, no. 012086 (2018): 1–7. Available from: http://dx.doi.org/10.1088/1757-899X/377/1/012086

[39] F.M. Tezel, O. Ozdemir, I.A. Kariper. "The Effects of pH on Structural and Optical Characterization of Iron oxide Thin Films." *Surface Review and Letters* 24, no. 4 (2017): 1-10. Available from: https://doi.org/10.1142/S0218625X17500512

[40] H.D. Cullity, S.R. Stock. "Element of X – ray Diffraction." 3rd Edition, Prentice Hall Publisher, New Jersey, USA. 2001.

[41] L.N. Ezenwaka, A.N. Nwori, I.E. Otti, N.A. Okereke, N.L. Okoli. "Investigation of the Optical, Structural and Compositional Properties of Electrodeposited Lead Manganese Sulfide (PbMnS) Thin Films for Possible Device Applications." *Nanoarchitectonic* 3, no, 1 (2022): 18-32. Available from: https://doi.org/10.37256/nat.3120221226